J. COMBIN. MATH. COMBIN. COMPUT. 127a (2025) 8477--8497

Journal of Combinatorial Mathematics and Combinatorial Computing
www.combinatorialpress.com/jcmcc

Combinatorial Press

Investigating the hydrological effects of smart technologies in urban rain garden design: a case study

Jie Tian[1], Dongdong Gao[2,✉]

[1] Fine Arts & Design College, Minjiang University, Fuzhou, Fujian, 350108, China
[2] School of Urban Construction, Fuzhou Technology and Business University, Fuzhou, Fujian, 350108, China

ABSTRACT
This paper applies smart technologies to urban rain garden design and analyzes the hydrological effects based on urban smart rain garden technologies. The SWMM model is used to simulate runoff water quantity and quality under the environment of long-term and continuous rainfall events in urban areas. Building area A is selected as the case study object of this paper, and its geographic location and precipitation data are analyzed to preliminarily explain the hydrological conditions of the case study area. Based on the SWMM model, the model pipe network generalization and other operations are carried out to establish the SWMM model of the study area. The SWMM model is calibrated in terms of the calibration of the model's parameters and the feasibility of the structured network SWMM model to verify the validity of the SWMM model of the study area and its catchment delineation method. Based on the urban smart rain garden technology, the LID module is added to the SWMM model of the study area and the hydrological effects under different scenarios such as combined LID are analyzed. Each LID measure can have a certain reduction effect on the combined runoff coefficient and total runoff. The combined LID measures in this paper have the best reduction effect, with the reduction rate of the integrated runoff coefficient over 35% and the total runoff over 50% in the 2h rainfall event. The combined LID scheme has the best reduction effect on the flood peak, and the reduction rate can reach more than 40% in both 2h rainfall events.

Keywords: smart technology, SWMM model, pipe network generalization, combined runoff coefficient, hydrological effect

1. Introduction

Rain gardens are engineering facilities with plants such as shrubs, flowers and even trees in low-lying areas, which mainly purify rainwater through the filtering effect of soil and plants, and at the same time reduce runoff by temporarily retaining rainwater and then slowly infiltrating it into the soil [1-3].

✉ Corresponding author.
E-mail address: 2160@mju.edu.cn (D. Gao).
Received 15 January 2024; Revised 25 March 2024; Accepted 30 November 2024; Published Online 15 April 2025.
DOI: 10.61091/jcmcc127a-468
© 2025 The Author(s). Published by Combinatorial Press. This is an open access article under the CC BY license (https://creativecommons.org/licenses/by/4.0/).

It is one of the technologies in the urban stormwater best management practices, and has been widely used in many developed countries in recent years for stormwater flood control and runoff pollution control systems, as well as an ecological type of indirect rainwater utilization facility [4-6]. Generally speaking, rain gardens can be constructed on various types of soil such as clay, sand, etc. They are mainly applicable to the periphery of buildings, parking lots, roads, etc. in urban public buildings, residential areas, commercial areas, and industrial zones, and they are also suitable for treating and utilizing rainwater runoff from decentralized buildings such as villa areas, tourist eco-villages, etc., as well as from newly-built villages and towns [7-10].

Hydrological effect refers to the influence of natural elements such as climate, topography and soil on the water cycle. It is a science that studies the cycling process of water on earth and its interaction with other earth systems, involving water storage, transportation and distribution [11-14]. Hydrological effects are important for our understanding and prediction of important issues such as water utilization, floods and droughts. Hydrological effects are mainly manifested through the recharge effect of precipitation and the generation of runoff. When precipitation occurs, a portion of the precipitation passes through the soil surface and enters the ground, replenishing groundwater resources [15-18]. This recharge plays an important role in maintaining the groundwater level, supporting agricultural irrigation, urban water supply and ecosystem stability.

This paper is a preliminary investigation of the important role of smart technology in urban rain garden design through its application program in urban rain garden design. A SWMM model is established based on the computation of sub-catchment generalization, surface yield, surface catchment and pipe network catchment models, which is used to simulate the runoff water quantity and water quality in the environment of rainfall events for the selected case study area. Building Area A located in Wuxi City, Jiangsu Province, is taken as the case study object of this paper, and rainfall data synthesized from the Chicago rainfall pattern is used as the rainfall sequence of the model to show the hydrological condition of the study area at the geographic location. The SWMM model of the study area is established by model pipe network generalization and catchment area generalization, and the results of model parameter calibration and structured network SWMM model feasibility test are given to verify the validity of the model constructed in this paper. According to the urban smart rain garden technology, the study area is designed, and the LID module is added on the basis of the SWMM model of the study area to analyze the hydrological effects of laying permeable pavement, depressed green space, grass planting, bioretention area and combined LID scheme alone. According to the influence of different urban rain garden design schemes on the runoff coefficient, total runoff and peak flow in the study area, we compare and analyze the hydrological effects of the urban rain garden design schemes applying smart technology in this paper.

2. Application of intelligent technology in urban rain garden design

2.1. Intelligent control

Intelligent control includes three parts: system network architecture, data transmission protocol, and control parameter setting. The system network architecture is constructed to utilize the data transmission of the microcontroller within the LAN and over the Internet via the LAN through the data chain layer, synchronous data chain control, and so on, thus realizing the setting and adjustment of the control parameters. The soil moisture sensor measures the humidity analog data, then processes the measured data and sends it to the microcontroller through a three-wire interface. When the detected humidity is less than the set humidity size, the system sends out instructions to control the pump to pump water for irrigation. When the detected humidity is equal to or higher than the set humidity level, the pump stops pumping water for irrigation.

2.2. End Sense

The end sensing system includes wireless sensor preference and deployment. Preferred wireless temperature sensors, wireless light sensors, according to the specific conditions of reasonable layout, build wireless intelligent end sensing system. Combined with the city management monitoring system, the reasonable deployment of urban garden green space camera. Through the information collection of the end sensing system, intelligent sensing prejudge the weather conditions, soil moisture and plant water demand in the next few days, prejudge the rainfall and rainwater accumulation situation, plant water shortage, and carry out intelligent and precise watering, so as to achieve the purpose of automation and intelligent control.

2.3. Water supply

The water supply in smart technology is divided into three categories, one is rainwater that has been stocked by rainwater harvesting systems. The second is urban reclaimed water. The third is local surface water or shallow groundwater, and the use of urban tap water is not advocated. Through the automatic water source switching device, the switching of irrigation water sources is carried out, making full use of modern IoT technology, optimizing the use of irrigation water sources such as rainwater harvesting, municipal water or other irrigation water, and implementing intelligent irrigation to achieve the purpose of further recycling rainwater resources and promoting water conservation.

2.4. Information management platform

The information management platform includes data management analysis and platform maintenance. Firstly, it establishes data platforms such as PC client and mobile APP, conducts surveys of selected objects on vegetation characteristics such as plant species, water demand period and fertility period, conducts surveys on irrigation conditions such as irrigation water quota, number of irrigation times and control methods of irrigation facilities, and on the basis of which, it refines the unit irrigation thresholds, carries out data entry and program writing, and establishes an information management platform. Secondly, the remote monitoring PLC system and camera observation are used to artificially adjust the water consumption, realize the monitoring of remote resources, upload real-time moisture data to the system, and set the thresholds in the system according to the demand of plants, and when the warning value is reached, start intelligent irrigation or release information notification.

3. Hydrological effects analysis model

3.1. Overview of the SWMM model

The SWMM model is mainly used to simulate runoff water quantity and quality in the environment of a single rainfall event in an urban area or to simulate a long-term and continuous process [19]. The runoff component of the model can effectively simulate rainfall runoff processes and pollution loads in the catchment area. The algorithmic component can simulate the process of runoff through pipe and canal, catchment facilities, and other network systems. It also tracks the changes in runoff water quality and quantity over multiple time periods in each study area and the process of water depth and flow changes in the drainage system.

3.2. SWMM model calculations

3.2.1. Subcatchment generalization. The SWMM model usually divides the study area into sub-catchments according to the nature of the subsurface and the characteristic parameters, and the sub-catchments are the hydrological response units of the SWMM model, which are used to calculate the runoff process respectively, and finally the flow superposition operation is carried out for each sub-catchment. Figure 1 shows the schematic diagram of a sub-catchment area, S_1 is the area of permeable area, S_2 is the area of storage impervious area, S_3 is the area of non-storage impervious area, L_1 is the sub-catchment characteristic width, which is also the characteristic width of permeable area, L_2 is the characteristic width of storage impervious area, and L_3 is the characteristic width of non-storage impervious area. The sub-catchment characteristic width is the ratio of the sub-catchment area to the longest path of surface diffuse flow, which is related as follows:

$$L_2 = \frac{S_2}{S_2 + S_3} L_1 \tag{1}$$

$$L_3 = \frac{S_3}{S_2 + S_3} L_1 \tag{2}$$

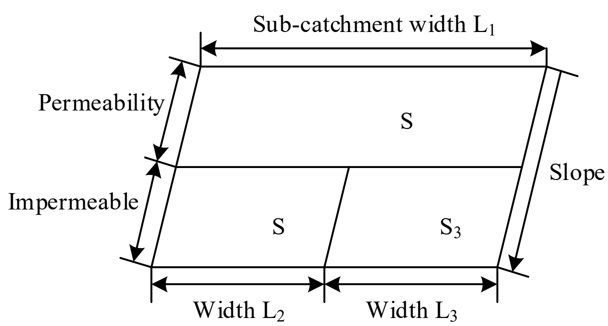

Fig. 1. Subcatchments generalization schematic diagram

3.2.2. Surface-produced flow modeling. As shown in Figure 1, the SWMM modeled sub-catchment runoff is each of three different types of surface runoff. The sum of the three parts of the outflow is the sub-catchment outflow.

1) Calculation of Surface Yield Flow in Permeable Area (Infiltration Model Calculation)

Rainfall first meets the surface infiltration process, when rainfall exceeds the amount of surface infiltration, the surface produces water storage, until more than the surface of the maximum storage capacity, surface runoff. The calculation formula is:

$$R_1 = (i - f)\Delta t \tag{3}$$

where, R_1 is the yield flow rate (mm).

i is the rainfall intensity (mm/h).

f is the infiltration rate (mm/h).

Δt is the rainfall duration (h).

The SWMM model provides three different computational models for simulating the process of infiltration of permeable zones within a sub-catchment, with an empirical model derived from the Horton model, which has a long history of application. The formulas are as follows:

$$f = f_\infty + (f_0 - f_\infty)e^{-kt} \tag{4}$$

where f is the infiltration rate (mm/min).

f_∞ is the stabilized infiltration rate (mm/min).

f_0 is the initial infiltration rate (mm/min).

k is the exponent of the reaction infiltration decay rate (s^{-1}).

t is the time (h).

The Green-Ampter model is a physical model based on Darcy's Law, which reflects the law of water infiltration in geotechnical voids. The model assumes that rainfall, in the process of infiltration, moves downward at a constant rate in the form of a wetting front (in the form of a soaking surface), and that no change occurs in the soil moisture and water-holding capacity above and below the wetting front as the wetting moves downward, and that the change in water content from the initial state to saturation in the wetting front occurs in a layer that is of negligible thickness. Based on the above assumed conditions, the following formula is derived:

$$F = \frac{K_S S_W \left(\theta_S - \theta_i\right)}{i - K_s} \tag{5}$$

where F is the cumulative infiltration depth of rainfall.

K_s is the saturated soil infiltration coefficient.

S_W is the soil water absorption at the infiltration surface.

θ_s is the saturated water content.

θ_1 is the initial water content.

i is the rainfall intensity (mm/h).

The numerical model of runoff curves was initially used to estimate the 24-hour natural rainfall in agricultural areas and later also used to calculate and analyze the flood flow process in urban areas. The runoff volume algorithm was determined as follows by taking into account the land use type, vegetation cover, rainfall, and initial soil saturation in the study area:

$$Q = \frac{\left(P - I_a\right)^2}{P - I_a + S} \tag{6}$$

where, Q is the actual net flow (mm).

P is the rainfall amount (mm).

I_a is the initial detention volume (mm).

s is the maximum potential retention (mm).

Where I_a is approximated by the formula: $I_a = 0.2S$. s can be determined by the parameter CN, which is a dimensionless empirical value used to reflect the comprehensive characteristics of the watershed before the rainfall event.

2) Calculation of surface-produced flow in the impoundment impervious area. When the storage impervious area experiences a rainfall process, the rainfall will produce surface runoff only after the maximum storage volume is satisfied in priority, and the runoff equation is expressed as:

$$R_2 = P - D \tag{7}$$

where, R_2 is the yield flow rate (mm).

P is the rainfall amount (mm).

D is the maximum water storage (mm).

3) Calculation of surface flow production in non-storage impervious areas. Evaporation process usually leads to non-storage impervious area rainfall suffered a small loss, in addition to the type of regional rainfall is basically all converted to surface runoff, the runoff formula is expressed as:

$$R_3 = P - E \tag{8}$$

where, R_3 is the amount of flow production (mm).

P is the rainfall (mm).

E is the evaporation (mm).

3.2.3. Surface catchment modeling. The three types of areas in the sub-catchment have runoff from each other and flow to the stormwater outfall as a representative catchment process.The SWMM model uses a nonlinear reservoir model to simulate the surface catchment process. The sub-catchment area is considered as a shallow reservoir with inflow from upstream runoff and rainfall, and outflow from evapotranspiration, infiltration, and stream production. The model assumes that the surface runoff at the outlet of the sub-catchment area is an approximately uniform flow form, and the relationship between its outflow and reservoir depth can be generalized to a nonlinear functional relationship with the continuity equation:

$$\frac{dV}{dt} = A\frac{dd}{dt} = Ai^* - Q \tag{9}$$

where v is the amount of surface water accumulation (m^3).

A is the area of sub-catchment (m^2).

d is the water depth (m).

i is the net rainfall intensity (m/s).

Q is the outflow $(\mathrm{m}^3/\mathrm{s})$.

The water flow rate in the sub-catchment area can be derived from Manning's equation:

$$Q = W\frac{1.49}{n}\left(d - d_p\right)^{\frac{5}{3}} \cdot s^{\frac{1}{2}} \tag{10}$$

where W is the sub-basin diffuse flow characteristic width (m).

n is the Manning's roughness coefficient.

d_p is the surface storage depth (m).

S is the sub-catchment slope (m).

3.2.4. Pipe network convergence modeling.Rainfall in the sub-catchment area eventually flows into the stormwater pipe network system after the surface flow generation and catchment process. The flow of rainwater into the network is a very complex hydrodynamic process. The SWMM model needs to be generalized to the pipe network system in the study area in order to simulate the process of rainfall entering the pipe network.The SWMM model provides three different computational models: constant flow, kinematic wave, and power wave.

The St. Venant system of equations describes the difference between the inflow at the inlet section and the outflow at the outlet section of the pipe, which is the volume increment of the water body in the pipe and can be described by the continuity equation:

$$\frac{\theta A}{\theta} + \frac{\theta Q}{\theta x} = q \tag{11}$$

Considering the energy difference between the upstream and downstream flow through the inlet and outlet sections, the energy equations can be obtained for the work done by the friction force and the work done by the acceleration force of the water flow, respectively:

$$\frac{1}{gA}\cdot\frac{\theta Q}{\theta t} + \frac{Q}{gA}\cdot\frac{\theta\frac{Q}{A}}{\theta x} + \frac{\theta h}{\theta x} - \left(S_0 - S_f\right) = 0 \tag{12}$$

where A is the cross sectional area of the converging pipe water flow $\left(m^2\right)$.

Q is the confluence pipe water flow rate $\left(m^3/s\right)$.

t is the time (s).

X is the length of the pipe along the water flow direction (m).

Q is the side inlet flow rate.

g is the gravitational acceleration.

h is the water depth (m).

S_0 is the bottom slope of the pipe.

S_f is the resistance slope drop.

The continuity equation and the energy equation are linked, which is the St. Vernand's system of equations, and the system of equations is solved to get the power wave solution, which is the power wave method. However, because the power wave method is more complicated and the process is more cumbersome, so according to the actual situation of the study area, the energy equation in the St. Vernand's equation system can be simplified and solved in conjunction with the continuity equation, i.e., the simplified form of the St. Vernand's equation. Among them, ignoring inertia and pressure, only considering the friction slope, that is, the kinematic wave method.

4. Case study regional hydrological modeling

4.1. Overview of the study area

4.1.1. Geographical location. Research object A building area is located in Wuxi City, Jiangsu Province, Wuxi is located in the south bank of the lower reaches of the Yangtze River, Taihu Lake Basin water network plain, located in the southern part of Jiangsu Province, the center of the Yangtze River delta, with the Yangtze River in the north, south of the Taihu Lake, looking east to the East China Sea, Shanghai, Nanjing, Hangzhou are equidistant from each other, and strangle the geographic hub of the south of the Yangtze River, and Suzhou, Wuxi, and linked together into a piece. Wuxi City belongs to the northern subtropical humid monsoon climate zone, with four distinct seasons, sufficient heat, abundant precipitation, rain and heat in the same season. The climate of Wuxi is mild and humid with abundant rainfall, belonging to the oceanic warm and humid climate zone in the lower reaches of the Yangtze River. According to the statistics of Wuxi Meteorological Station, the average annual precipitation is 1,087mm, and the average annual evaporation is 1,248.6mm. The general climate is characterized by the following features: winter is dominated by northerly winds, and it is attacked by cold air from the northern continent, which is dry and cold. In summer, the southeasterly wind is the dominant wind, influenced by the ocean monsoon, hot and humid. Among them, the spring and summer of the “rainy” weather is unique to the Jiangnan region's climate characteristics, hot, rainy weather, humidity. In late summer and early fall, the number of typhoons is high, and the combination of stormy weather often brings large precipitation, which is more destructive.A total area of the site of the construction area is 48,726 m^2, and the terrain of the proposed site is relatively flat, with no unfavorable topography and geomorphology, and the stability is relatively good, which is suitable for the construction of the project.

4.1.2. Rainfall data. Rainfall is necessary to generate surface runoff, and rainfall data, which can be defined in the model through rain gauges and temporal rainfall series, are essential for model construction. Usually the source of rainfall data is the measured rainfall data for a particular rainfall calendar time in the study area or the rainfall data for the area is designed and synthesized by the rain pattern method. The Chicago rain model is widely used in engineering design simulation because of the advantages of small error and good fit between the designed and synthesized rainfall process lines and the measured rainfall data, simple calculation and synthesis process, no dependence on local rainfall process data, and peak intensity is not affected by the rainfall calendar time. The short-calendar-time rainfall pattern usually adopts the Chicago rainfall pattern, and the short-calendar-time rainstorm is also more in line with the actual rainfall situation in the study area, so this paper adopts the rainfall data synthesized by the Chicago rainfall pattern as the rainfall sequence of the model.

Chicago rain type in the storm intensity formula [20] on the basis of the introduction of the rain peak ratio coefficient r to reflect the location of the peak rain intensity, the design of the synthetic rainfall process is first according to the rainfall calendar time is divided into two parts of the pre-peak and post-peak. Generally, the rain peak coefficient r is taken as 0.3-0.5, and the rain peak coefficient will be different in different regions where the spatial and temporal rainfall distribution is not used. The formula for rainstorm intensity is shown in equation (13):

$$q = \frac{4758.5 + 3089.5 \lg P}{(t + 18.469)^{0.845}} \tag{13}$$

Eq:

q - Design storm intensity $(L/s \cdot hm^2)$.

P - Rainfall return period (a).

t - Rainfall duration (min).

The rainfall return period is set to be P=2, 3, 5, 10, 20 and 50a, the rainfall peak coefficient r is taken as 0.5, and the rainfall duration t is taken as 120 min, and the rainfall process line of the above six return periods is generated by using the Chicago rain generator, and the specific rainfall data are shown in Table 1 and Fig. 2. As can be seen from Fig. 2, the rainfall intensities of different recurrence periods are monotonically increasing to the maximum peak and then monotonically decreasing with the increase of rainfall duration, and the corresponding rainfall intensities are larger with the increase of rainfall recurrence period. The rainfall intensity peaks at 57 min for all six rainfall return periods, which is consistent with the characteristics of the Chicago rain type single peak.

Table 1. Rainfall and peak rainfall intensity during 120min

Recurrence period P(a)	Rainfall amount(mm)	Peak rainfall intensity(mm/min)
2	62.138	2.836
3	68.749	3.078
4	75.268	3.514
10	83.254	3.983
20	97.463	4.384
50	109.772	5.271

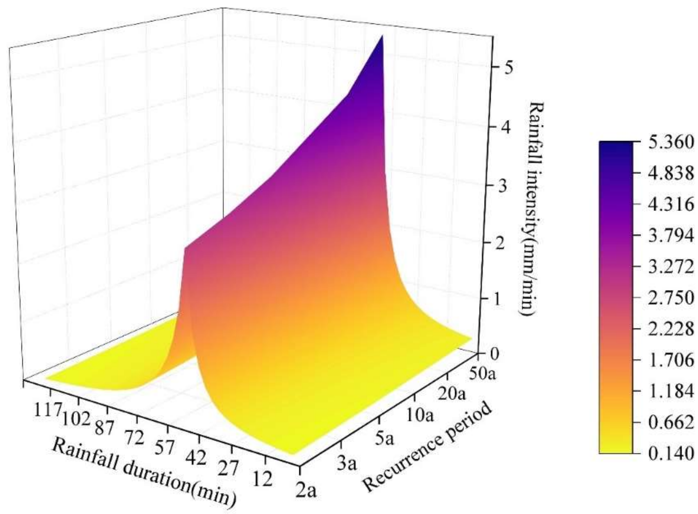

Fig. 2. Rainfall intensity of different recurrence period in 120min

4.2. SWMM modeling of the study area

4.2.1. Model pipe network generalization:

1) Pipe network generalization. The pipe network system in the SWMM model is the network of pipes connected by inspection wells. The pipe network data comes from the study area planning map, and the pipe network is generalized by extracting the spatial distribution characteristics of the pipe network of the drainage system in the study area. Specifically, the CAD plan of the stormwater pipe network is imported into the SWMM model, and based on the distribution of pipe connections in the plan, the system of stormwater wells (or inspection wells) and pipe networks is constructed as shown in Figure 3. In the process of pipe network generalization, if there is a sudden change in the shape, size and slope of the pipe network, according to the actual situation or assumptions to add check wells to reflect. The flow transfer calculation in the model is based on extracting the attribute data such as the length, diameter and flow direction of the pipe network, and then inputting them into the parameter attribute table of the pipe network. The parameters to be inputted for the inspection wells include: location coordinates, top and bottom elevations, depth, initial water depth, and overflow depth. The input parameters for stormwater pipes include: pipe length, pipe roughness, pipe diameter, pipe slope, and cross-section shape.

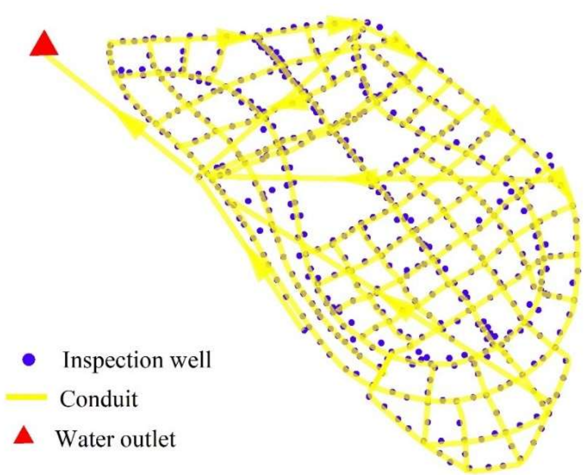

Fig. 3. Generalization of the pipeline network in the research area

The network generalization for Building Area A is specifically 598 inspection wells and 593 storm drains. The material of the stormwater wells is concrete basically located on both sides of the street. The surface elevation was obtained from the DEM digital elevation map downloaded from the geospatial data cloud. The burial depth of the stormwater pipes at 1.2m below the surface of the stormwater wells at the very front of the network. The elevation of the bottom of the stormwater well at 50 cm below the outer bottom of the drain pipe and the elevation of its inner bottom is the pipe bottom elevation. The slope of the drain pipe is 0.3%. The bottom elevation of the inlet pipe of the stormwater well is 15 cm higher than the bottom elevation of the outlet pipe.The drain pipe is made of concrete and has a circular cross-sectional shape with a diameter between 0.5 m and 2.5 m. The drain pipe has a roughness of the inner wall and a roughness of the outer wall of the pipe. The inner wall roughness of the concrete pipe is taken as 0.016. The properties of some of the inspection wells are shown in Table 2 and the properties of the drainage pipes are shown in Table 3.

Table 2. Partial inspection well attributes

Well number	Bottom elevation(m)	Surface elevation(m)	Well depth(m)	Initial water depth(m)
J1	1.8	4.3	2.6	0
J2	1.3	4.1	2.9	0
J3	1.7	4.8	2.1	0
J4	2.0	4.2	2.4	0
J5	0.5	3.4	2.8	0

Table 3. Patrial rainwater pipeline attributes

Pipe number	Import inspection well	Export inspection well	Length(m)	Roughness	Diameter(m)
P1	J4	J3	128	0.016	0.8
P2	J2	J1	104	0.016	1.2
P3	J3	J2	132	0.016	0.9
P4	J1	J5	171	0.016	1.3
P5	J5	J6	164	0.016	1.6
P6	J6	J7	158	0.016	1.4

2) Establishment of pumping stations. Four stormwater pumping stations were established in Building A, namely the northern pumping station, the southern pumping station, the southwestern pumping station and the eastern pumping station. The rainwater pumps of the four pumping stations are axial flow pumps. The rainwater pump model of the northern pumping station is ZLB2.8-6.7, the rainwater pump model of the southern pumping station is 900ZLB-70(-2°), the rainwater pump model of the southwestern pumping station is ZLB2.8-6.7, and the rainwater pump model of the eastern pumping station is ZL3670-6(-4°)-280.The detailed information of the rainwater pumps is shown in Table 4, in which Q is the flow rate of the rainwater pumps, and H is the rainwater pump head. According to the rainwater pump model to find the rainwater pump flow level relationship shown in Table 5. The data in Table 4 reflects that with the increasing head H of the rainwater pump, the flow rate Q of the rainwater pump shows a decreasing trend.

Table 4. Rainwater pump details

Pump station name	Q(m^3/h)	H(m)	Speed of revolution(r/min)	Distribution power(Kw)
North rainwater pump	9328.0	8.26	450	220
Southern rainwater pump	5438.2	6.78	450	220
Southwest rainwater pump	8769.8	7.42	450	220
Eastern rainwater pump	9547.4	7.83	450	220

Table 5. Rainwater pump performance value

North rainwater pump		Southern rainwater pump		Southwest rainwater pump		Eastern rainwater pump	
H(m)	Q(m^3/h)	H(m)	Q(m^3/h)	H(m)	Q(m^3/h)	H(m)	Q(m^3/h)
4.35	3.83	2.83	2.73	4.44	3.67	4.40	3.66
4.87	3.67	3.04	2.45	4.55	3.56	4.72	3.61
5.01	3.40	3.54	2.32	5.26	3.47	5.44	3.45
5.95	3.35	4.44	2.30	5.87	3.40	5.87	3.40
6.43	3.21	4.91	2.09	6.04	3.36	6.03	3.36
6.52	3.14	5.40	2.03	6.84	3.06	6.64	3.20
7.25	3.06	5.65	1.91	7.32	2.94	7.09	3.18
7.96	2.80	6.06	1.86	7.54	2.91	7.91	3.02
8.04	2.71	6.63	1.77	8.31	2.50	8.18	2.97

4.2.2. Catchment Area Generalization:

1) Catchment delineation. The sub-catchment delineation of Building Area A is performed based on the ArcGIS tool using the SWMM model catchment delineation method described in the previous section. The catchment surface of Building Area A delineated using the structured grid approach is shown in Figure 4. After structured grid delineation, effective grid screening was performed based on the area and boundary extent of the study area.

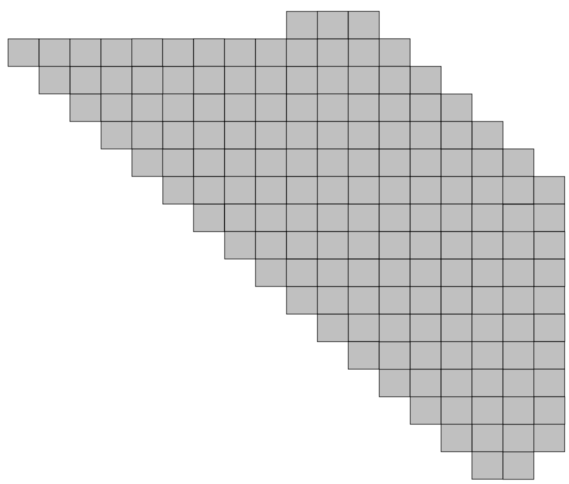

Fig. 4. Structured network

2) Catchment parameters. The parameters of sub-catchment area include coordinates, area, runoff outlet and so on. Parameters take the value of the status of the surface of the slope to take 0.3%, impermeable area Manning coefficient to take 0.016, permeable area Manning coefficient to take 0.35, impermeable area puddle depth of 2mm, permeable area puddle depth of 8mm, impermeable area does not contain the waterlogged puddle area of the percentage of 0. The length of the catchment refers to the sub-catchment area of the distance from the runoff collection check wells the farthest distance. The catchment length is the furthest distance from the runoff collection check well in the sub-catchment. Since the sub-catchments have the same shape and size, the catchment length of the sub-catchments is the same. The Ruler command in the model can be used to calculate the catchment length of the sub-catchments. Once the catchment length is determined, the model automatically calculates the subcatchment width, which is the area divided by the catchment length.

4.2.3. Model calibration. The SWMM model calibration is divided into two parts, one is the parameter calibration of the model, and the other is the feasibility verification of the structured network SWMM model.

1) Calibration of model parameters. By running the SWMM model under calibrated rainfall, the integrated runoff coefficient of the study area is calculated, and this coefficient is compared with the runoff coefficient calibration target to determine the direction of parameter adjustment. When the simulated runoff coefficient is less than the empirical value of the calibration target, the runoff volume generated in the catchment area is increased by adjusting the parameters to be calibrated in the SWMM model. When the simulated runoff coefficient value was greater than the calibration empirical value, the parameters to be calibrated were adjusted in the opposite direction of the model to reduce the amount of runoff from the catchment. After repeated adjustments and re-simulations, the model parameters when the target empirical value of runoff coefficient is satisfied are finally determined, and the specific results are shown in Table 6. Since the average imperviousness of building area A in this study is 75.49%, and checking the table of empirical values of integrated urban runoff coefficients shows that the study area belongs to a densely built-up center, the target runoff coefficients are calibrated to be between 0.6 and 0.8. After calibrating the rainfall model runs and adjusting the parameters, the final parameters are obtained as shown in Table 7. The validated rainfall model was run to obtain a composite runoff coefficient of 0.69 for the 1-year event and 0.78 for the 5-year event, both simulated values were within the target composite runoff coefficient.

Table 6. Empirical value of urban integrated runoff coefficient

Regional condition	Integrated runoff coefficient
Dense central area of buildings(impermeable coverage area:>70%)	0.6~0.8
Central area with denser buildings(impermeable coverage area:50%~70%)	0.5~0.7
Central area with sparse buildings(impermeable coverage area:30%~50%)	0.4~0.6
Central area which is almost no buildings(impermeable coverage area:<30%)	0.3~0.5

Table 7. Model runoff coefficient

Calibration parameter	1a_2h	5a_2h
Non-permeable manning coefficient	0.016	0.016
Permeability manning coefficient	0.27	0.26
Non-permeable storage(mm)	1.54	1.52
Permeable storage(mm)	5.83	5.96
Suction head(mm)	289.04	291.83
Conductivity(mm/h)	0.54	0.57
Initial loss	0.217	0.224
Simulated regional integrated runoff coefficient value	0.69	0.78
Integrated runoff coefficient	0.6-0.8	

2) Structured network SWMM model validation. In order to verify the model simulation results using the structured grid division method, the water depth of the drainage outlet in the simulation results of the model is evaluated, the model sub-catchment division results and the scatter plot of the model simulation results are shown in Figures 5 and 6, and the evaluation indicators of the simulation results are shown in Table 8. The 2017 historical rainfall scenario was used as the calibration scenario, and the evaluation indicators were selected as correlation coefficient, Nash-Sutcliffe coefficient, and estimated standard error. The evaluation indexes of the drainage outlet depth data of the computational model are correlation coefficient 0.962, Nash-Sutcliffe coefficient 0.853, and estimated

standard error 0.024. The evaluation indexes of the model's infiltration data are correlation coefficient 0.984, Nash-Sutcliffe coefficient 0.928, and estimated standard error 0.037, which is credible, and it proves that the structured grid delineation method is feasible.

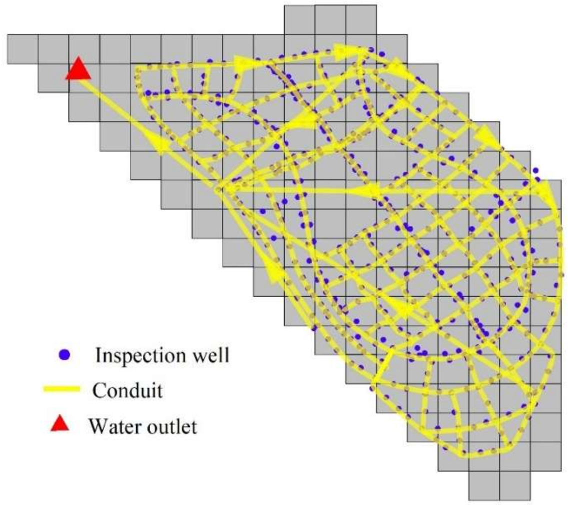

Fig. 5. Division results of model sub catchment areas

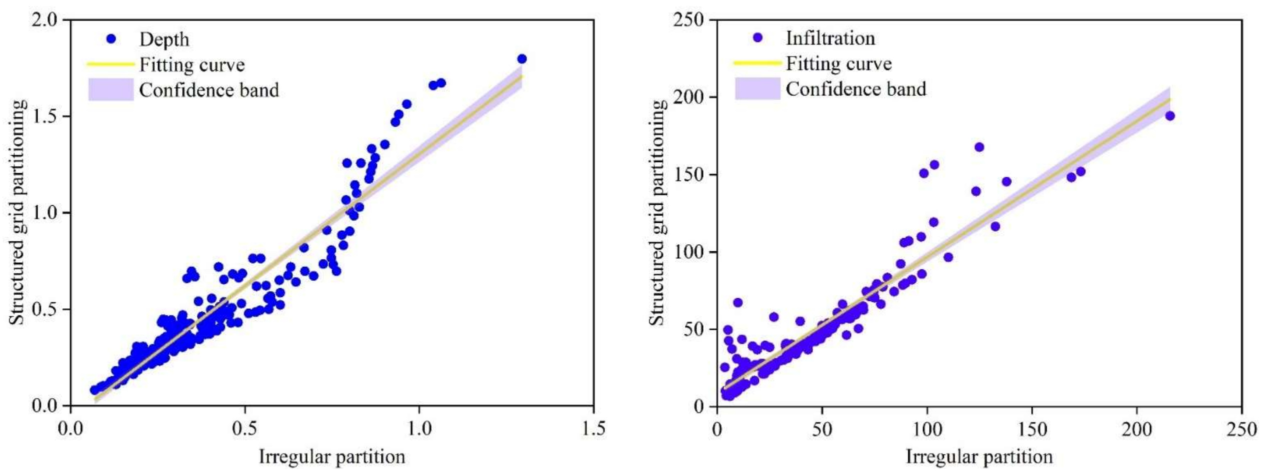

(a) Drainage depth(m)

(b) Total infiltration(mm/h)

Fig. 6. Model simulation results

Table 8. Model results evaluation index

Index	Drainage depth	Total infiltration
Nash-sutcliffe coefficient	0.853	0.928
Correlation coefficient	0.962	0.984
Estimated standard error	0.024	0.037

5. Analysis of hydrological effects in the case study area

The study area is designed according to the urban smart rain garden technology, with four development measures: permeable paving, depressed green space, grassed swales, and bioretention areas. The design utilizes the natural drainage system instead of the conventional stormwater pipelines, and the flow is converged through the grassed swales, retention and diversion swales, roadside ditches, and bioretention areas, and then discharged from the municipal pipelines. In this section, the LID module is added to the SWMM model of the study area in the previous section to verify the feasibility of this catchment scheme and to analyze the hydrological effects of laying permeable paving, undercut green space, grassed swales, bioretention areas and combined LID schemes individually.

5.1. Case Study Area LID Program Settings

5.1.1. LID measures and parameter selection. According to the design of urban smart rain garden development technology in the study area, a total of four LID measures [21] were selected to achieve the control objectives of reducing the total amount of runoff, flood flow, delaying the peak emergence time, shortening the ponding time, and reducing the total amount of ponded water, which are permeable paving, undercutting green space, grass-planting ditch, and bioretention area. According to the results of the permeable paving physical experiment and the construction design of the study area, the parameters of LID measures were selected as shown in Table 9.

Table 9. LID measure parameter value

LID measure	Structural layer	Design parameter	Parameter value	Recommended value
Water float	Surface layer	Depth of storage(mm)	4.82	\
		Surface roughness	0.13	0.13
		Surface slope/%	80.46	100-120
	Pavement layer	Thickness/mm	0.57	0.20-0.60
		Pore ratio	250.73	\
	Aquifer	Permeability(mm·h^{-1})	348.26	150-450
		Thickness/mm	0.47	0.45-0.75
		Pore ratio	148.94	\
Lower green space	Surface layer	Depth of storage(mm)	0.16	0.10-0.20
		Surface roughness	1.03	\
		Surface slope/%	0.92	\
	Soil horizon	Thickness/mm	399.47	400-450
		Pore ratio	0.53	0.5-0.6
Grass trench	Surface layer	Depth of storage(mm)	19.86	\
		Surface roughness	0.17	0.15-0.20
		Surface slope/%	0.94	\
		Slope ratio	3.48	\
Biological retention area	Surface layer	Depth of storage(mm)	594.38	\
		Surface roughness	0.14	0.10-0.15
		Surface slope/%	0.23	\
	Soil horizon	Thickness/mm	400.06	350-500
		Pore ratio	0.49	0.4-0.5
	Aquifer	Thickness/mm	148.73	100-150
		Pore ratio	0.66	0.5-1.0

5.1.2. Model Scenario Setup. A total of seven scenarios are set up for SWMM model simulation, as shown in Table 10. Among them, Scenario 1 is a conventional development scenario with no LID measures as a control group. Scenario 2 is a combination of 4 LID measures, with 17% of the area occupied by permeable pavement, 5% of the area occupied by undercroft, 4% of the area occupied by grass swales, and 2% of the area occupied by bioretention area, in which the permeable pavement is the original impervious parking lot, and the remaining 3 LID measures are converted from ordinary grass. Option 3 is based on Option 2 to lay rainwater wells and rainwater pipes in the corresponding locations, change the sinking method to the sinking of rainwater pipe network, and compare and analyze the possibility of replacing the sinking of rainwater pipe network by grass-planting ditch and roadside ditch, as well as the advantages and disadvantages of the two. Scenarios 4 to 7 are the combination of the LID scheme of permeable paving, depressed green space, grassing ditch, bioretention area alone, the parameters used and the parameters of Scenarios 2 and 3 to maintain consistency, in order to analyze the impact of the individual and combination of each LID measures on the hydrological effects of the study area.

Table 10. SWMM model scheme setting

<table>
<tr><th>Serial number</th><th>Scheme</th><th colspan="2">LID measure ratio/%</th><th>Remittance mode</th></tr>
<tr><td>1</td><td>Conventional development</td><td colspan="2">0</td><td>Water pipe net</td></tr>
<tr><td rowspan="4">2</td><td rowspan="4">Combination LID</td><td>Water float</td><td>17</td><td rowspan="4">Through the planting of the grass trench, the rainwater flows</td></tr>
<tr><td>Lower green space</td><td>5</td></tr>
<tr><td>Grass trench</td><td>4</td></tr>
<tr><td>Biological retention area</td><td>2</td></tr>
<tr><td rowspan="4">3</td><td rowspan="4">Combination LID</td><td>Water float</td><td>17</td><td rowspan="4">Water pipe net</td></tr>
<tr><td>Lower green space</td><td>5</td></tr>
<tr><td>Grass trench</td><td>4</td></tr>
<tr><td>Biological retention area</td><td>2</td></tr>
<tr><td>4</td><td>Water float</td><td colspan="2">17</td><td>Water pipe net</td></tr>
<tr><td>5</td><td>Lower green space</td><td colspan="2">5</td><td>Water pipe net</td></tr>
<tr><td>6</td><td>Grass trench</td><td colspan="2">4</td><td>Water pipe net</td></tr>
<tr><td>7</td><td>Biological retention area</td><td colspan="2">2</td><td>Water pipe net</td></tr>
</table>

5.2. Analysis of hydrological effects

5.2.1. Runoff Coefficient and Total Runoff. The SWMM model simulates the rainfall runoff process of seven scenarios under different rainfall return periods and two rainfall durations. The integrated runoff coefficients and total runoff amounts for different scenarios of 2h and 24h rainfall are simulated, and the integrated runoff coefficient reduction rates and total runoff reduction rates for different scenarios are thus statistically calculated, and the specific results are shown in Figs. 7 and 8, which represent the integrated runoff coefficients and the changes in their reduction rates for t=2h and t=24h, respectively, and the total runoff amounts and their changes in the reduction rates for t=2h and t=24h, respectively. The total runoff and its reduction rate changes for t=2h and t=24h are shown in Fig. 8(a) and (b), respectively, and IRC, RT and RR denote the integrated runoff coefficient, the total runoff and the reduction rate, respectively, and S1-S7 denote the seven different scenarios. From the data in the figure, it can be seen that each LID measure can play a certain role in reducing the integrated runoff coefficient and the total amount of runoff, and the combined LID measures based on the urban intelligent rain garden design technology in this paper have the best reduction effect, with the reduction rate of the integrated runoff coefficient over 35% and the total amount of runoff over 50% in the 2-h rainfall event. The reduction effect is weakened in the 24-h rainfall event, but the reduction effect of the combined LID measures on the integrated runoff coefficient and the total amount of runoff is weaker. The reduction effect of the 24h rainfall event is weaker, but the reduction rate of the combined LID measures is still more than 21% for the combined runoff coefficient and more than 34% for the total runoff.

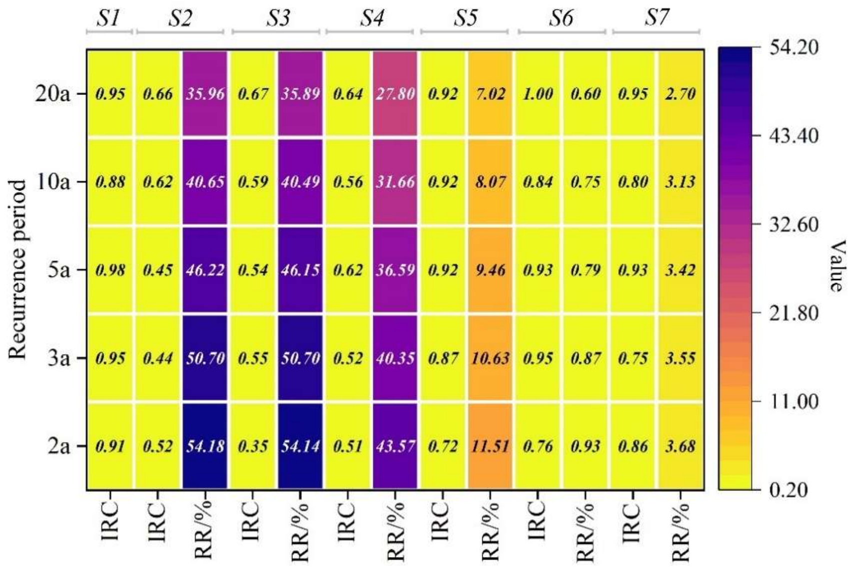

(a) The total runoff coefficient of 2h and its reduction rate

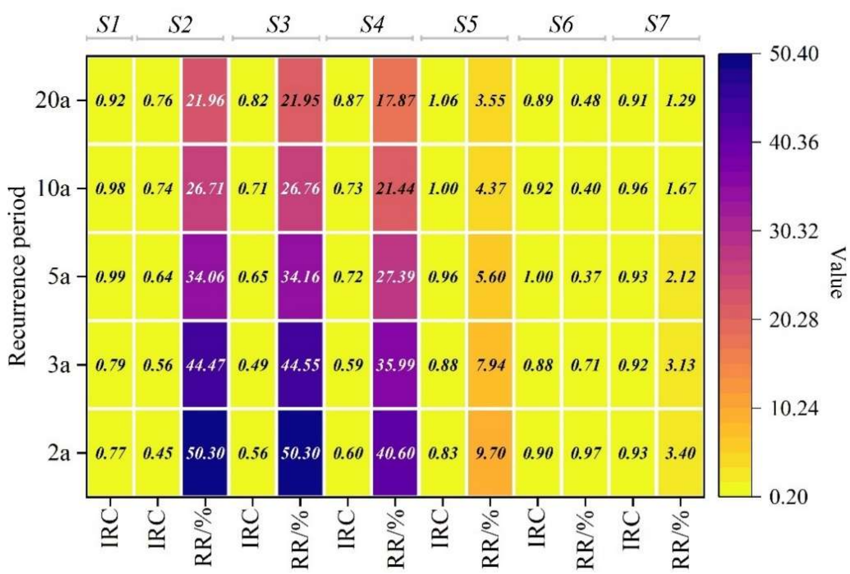

(b) The total runoff coefficient of 24h and its reduction rate

Fig. 7. The integrated runoff coefficient and its reduction rate vary

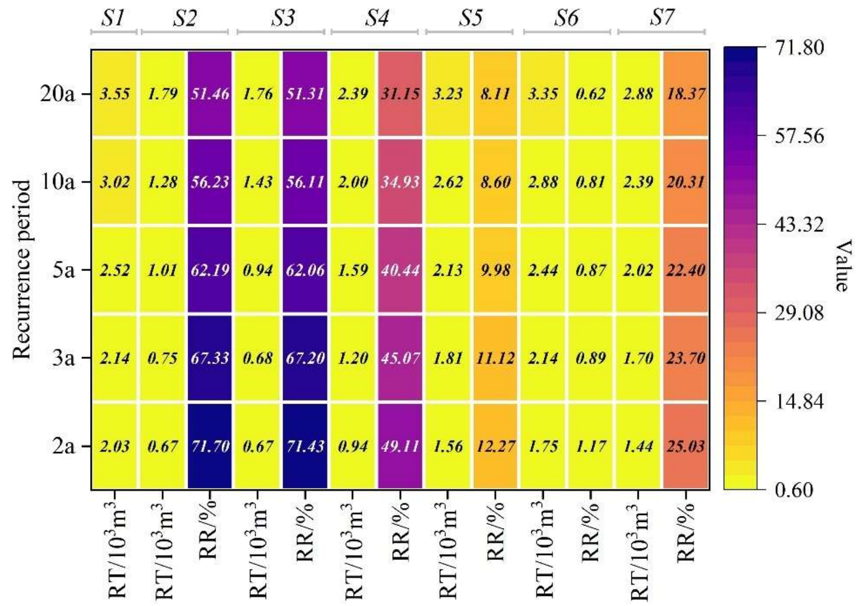

(a) The runoff total of 2h and its reduction rate

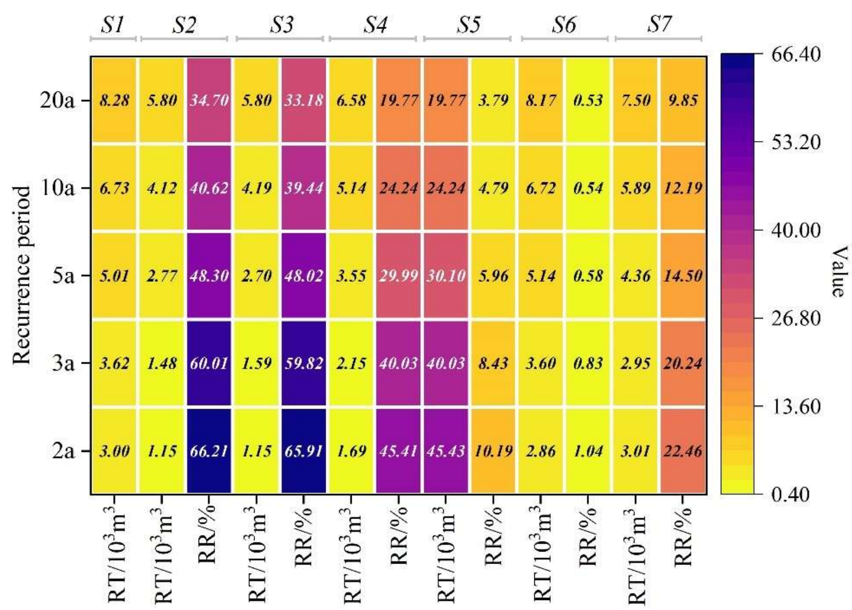

(b) The runoff total of 24h and its reduction rate

Fig. 8. The runoff total and its reduction rate vary

5.2.2. Flood flows. There are 46 sub-basins in the study area, of which 44 sub-basins are discharged from OUT1 and only 2 sub-basins are discharged from OUT2, which have smaller flow and basically no LID measures within the confluence, so the flood peak situation and flow process of OUT1 are mainly analyzed. The simulation results of OUT1 peak flow and the corresponding peak flow reduction rate are shown in Fig. 9, where PD indicates the peak flow, RR indicates the reduction rate, and S1-S7 indicate the different scenarios. From the figure, it can be seen that each LID measure can reduce the flood flow to some extent. In the case of the same rainfall return period, the reduction rate of the flood peak flow of each scheme for 2h rainfall is generally greater than that for 24h rainfall, and the combined LID scheme based on the urban smart rain garden technology has the best reduction effect on the flood peak, and the reduction rate can reach more than 40% in the case of 2h rainfall, and in the case of 24h rainfall, only the rate of the reduction rate in the case of the return period of the hour is more than 40%, and the reduction decreases sharply after that.

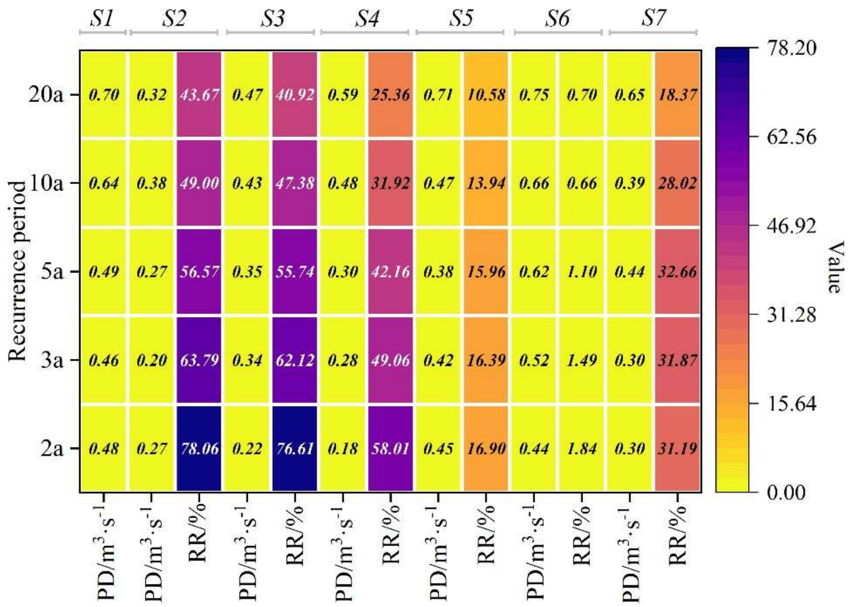

(a) The peak discharge of 2h and its reduction rate

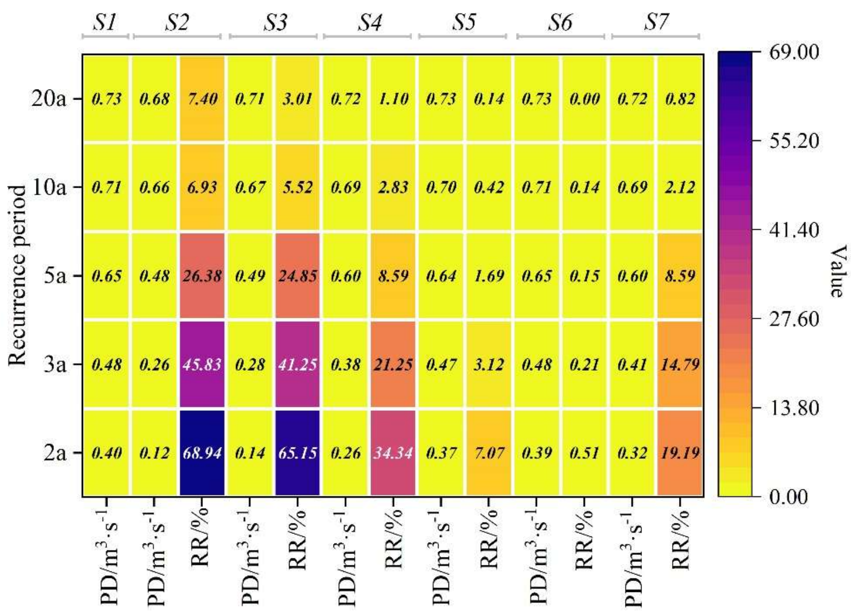

(b) The peak discharge of 24h and its reduction rate

Fig. 9. The peak discharge and its reduction rate vary

6. Conclusion

In this paper, smart technology is applied to design urban rain garden layouts, and hydrological simulation of the case study area is carried out through the SWMM model. The calculation results of runoff coefficient, total runoff volume and flood flow in the study area under different scenarios are analyzed, so as to highlight the hydrological effect of smart technology on urban rain garden design. The study shows that each LID measure can play a certain role in reducing the integrated runoff coefficient and the total amount of runoff, and the combined LID measures based on the urban smart rain garden design technology in this paper have the best reduction effect, with the integrated runoff coefficient reduction rate of more than 35% and the total amount of runoff reduction rate of more than 50% in the 2-h rainfall event. 24-h rainfall event kind of reduction effect is weakened, but the reduction rate of the combined LID measures on the integrated runoff coefficient is still higher than the total amount of runoff in the 24-h rainfall event. The reduction effect of the 24h rainfall event is weakened, but the reduction rate of the combined LID measures on the integrated runoff coefficient is still more than 21%, and the reduction rate on the total runoff is more than 34%. At the same time, the combined LID scheme based on urban smart rain garden technology has the best reduction effect on flood peaks, and the reduction rate can reach more than 40% for 2h rainfall, and only the reduction rate of the reproduction period is more than 40% for 24h rainfall, and the reduction rate decreases sharply after that. It is fully explained that the application of intelligent technology in urban rain gardens can effectively reduce the urban runoff coefficient, the total amount of runoff and the flood peak flow, alleviate the flooding problem that exists prominently in the construction and development of the city, and provide a new way of thinking for urban planning and construction.

Acknowledgements

This paper was supported by the research project of Fuzhou Science and Technology Association in 2024, "Suggestions on Improving the resilience prevention and control system of flood control and drainage in Fuzhou Urban Area".

References

[1] Sharma, R., & Malaviya, P. (2021). Management of stormwater pollution using green infrastructure: The role of rain gardens. Wiley Interdisciplinary Reviews: Water, 8(2), e1507.

[2] Zhang, L., Ye, Z., & Shibata, S. (2020). Assessment of rain garden effects for the management of urban storm runoff in Japan. Sustainability, 12(23), 9982.

[3] Ishimatsu, K., Ito, K., Mitani, Y., Tanaka, Y., Sugahara, T., & Naka, Y. (2017). Use of rain gardens for stormwater management in urban design and planning. Landscape and Ecological Engineering, 13, 205-212.

[4] Yuan, J., Dunnett, N., & Stovin, V. (2017). The influence of vegetation on rain garden hydrological performance. Urban Water Journal, 14(10), 1083-1089.

[5] Burszta-Adamiak, E., Biniak-Pieróg, M., Dąbek, P. B., & Sternik, A. (2023). Rain garden hydrological performance–Responses to real rainfall events. Science of the Total Environment, 887, 164153.

[6] Autixier, L., Mailhot, A., Bolduc, S., Madoux-Humery, A. S., Galarneau, M., Prévost, M., & Dorner, S. (2014). Evaluating rain gardens as a method to reduce the impact of sewer overflows in sources of drinking water. Science of the Total Environment, 499, 238-247.

[7] Church, S. P. (2015). Exploring Green Streets and rain gardens as instances of small scale nature and environmental learning tools. Landscape and Urban Planning, 134, 229-240.

[8] Schlea, D., Martin, J. F., Ward, A. D., Brown, L. C., & Suter, S. A. (2014). Performance and water table responses of retrofit rain gardens. Journal of Hydrologic Engineering, 19(8), 05014002.

[9] Hess, A., Wadzuk, B., & Welker, A. (2019). Predictive evapotranspiration equations in rain gardens. Journal of Irrigation and Drainage Engineering, 145(7), 04019010.

[10] Nichols, W. (2018). Modeling performance of an operational urban rain garden using HYDRUS-1D. Villanova University.

[11] Cristiano, E., ten Veldhuis, M. C., & Van De Giesen, N. (2017). Spatial and temporal variability of rainfall

and their effects on hydrological response in urban areas–a review. Hydrology and Earth System Sciences, 21(7), 3859-3878.

[12] Karlsson, I. B., Sonnenborg, T. O., Refsgaard, J. C., Trolle, D., Børgesen, C. D., Olesen, J. E., ... & Jensen, K. H. (2016). Combined effects of climate models, hydrological model structures and land use scenarios on hydrological impacts of climate change. Journal of Hydrology, 535, 301-317.

[13] Zhao, L., Zhang, T., Li, J., Zhang, L., & Feng, P. (2023). Numerical simulation study of urban hydrological effects under low impact development with a physical experimental basis. Journal of Hydrology, 618, 129191.

[14] Pavlovskii, I., Hayashi, M., & Itenfisu, D. (2019). Midwinter melts in the Canadian prairies: energy balance and hydrological effects. Hydrology and Earth System Sciences, 23(4), 1867-1883.

[15] Brotherton, S. J., Joyce, C. B., Berg, M. J., & Awcock, G. J. (2019). Immediate and lag effects of hydrological change on floodplain grassland plants. Plant Ecology, 220, 345-359.

[16] Guan, M., Sillanpää, N., & Koivusalo, H. (2015). Modelling and assessment of hydrological changes in a developing urban catchment. Hydrological Processes, 29(13), 2880-2894.

[17] Baker, H. J., Hutchins, M. G., & Miller, J. D. (2021). How robust is the evidence for beneficial hydrological effects of urban tree planting?. Hydrological Sciences Journal, 66(8), 1306-1320.

[18] Zhang, J., Song, X., Wang, G., HE, R., & WANG, X. (2014). Development and challenges of urban hydrology in a changing environment: I: Hydrological response to urbanization. Advances in Water Science, 25(4), 594-605.

[19] L M Najib,N Bateni & D Y Seng Mah. (2024). Assessment of the sub-urban drainage system resilience on the increased flooding scenario using Storm Water Management Model (SWMM). IOP Conference Series: Earth and Environmental Science(1),

[20] Liu Xingpo,Ouyang Chenmeng & Zhou Yuwen. (2022). A Low-Return-Period Rainfall Intensity Formula for Estimating the Design Return Period of the Combined Interceptor Sewers. Water Resources Management(1),289-304.

[21] Chengguang Lai,Yifan Luo,Xuefang Li,Haijun Yu,Zhaoyang Zeng,Shanshan Li... & Zhaoli Wang. (2024). Assessment on vulnerability of road networks considering the dynamic impact of urban waterlogging and the mitigation effect of LID measures. Journal of Hydrology132005-132005.